Analyst

PAPER

View Article Online
View Journal

Cite this: DOI: 10.1039/d0an00035c

Rapid screening and quantitative detection of *Salmonella* using a quantum dot nanobead-based biosensor†

Jiao Hu, *[a,c] Feng Tang,[d] Yong-Zhong Jiang[e] and Cui Liu *[b]

Received 7th January 2020,
Accepted 10th February 2020

DOI: 10.1039/d0an00035c

rsc.li/analyst

The continuing hurdle of developing foodborne pathogen detection techniques is that compromises must be made among simplicity, portability, speed, sensitivity, and quantitation. Herein, we fabricated quantum dot nanobeads (QDNS) by a layer-by-layer assembly of quantum dots on the surface of polymer nanospheres. QDNS exhibited higher fluorescence intensity than the quantum dots at the same particle number. Based on the quantum dot nanobeads as the signal reporter, a quantitative lateral flow immunoassay was demonstrated for *Salmonella typhimurium* detection with improved sensitivity, specificity and accuracy. A visual detection limit of 5×10^3 CFU mL^{-1} *Salmonella typhimurium* within 10 min has been proved and demonstrated. Additionally, higher concentrations of non-*Salmonella typhimurium* bacteria have negligible effects on the detection of *Salmonella typhimurium*. The results of 50 single blind tests by 10 testers suggested that the assay exhibited 100% accuracy. The results illustrate that the assay provides a balance among simplicity, speed, sensitivity and accuracy, and it can be a favorable alternative for *Salmonella typhimurium* screening in various samples.

Introduction

Infectious diseases caused by foodborne pathogens are one of the greatest threats to human health.[1,2] In 2016, the Foodborne Diseases Active Surveillance Network (Food Net) confirmed 24 029 illnesses, 5512 hospitalizations, and 98 deaths.[3] In addition, the number of foodborne pathogen infections increased dramatically in 2016 compared to the average of those in 2013–2015. The incidence of foodborne pathogen infections per 100 000 is the highest for *Salmonella*, which is 7277 per 100 000 individuals among all the pathogens.[4,5] In 2017, the Centers for Disease Control and Prevention (CDC) and public health officials in several states identified a multi-state outbreak of *Salmonella typhimurium* infections in America.

To date, several available and convenient methods for foodborne pathogen detection have been reported,[6] including traditional culture-based methods,[7,8] enzyme-linked immunosorbent assay (ELISA),[9] polymerase chain reaction (PCR),[10] and other electrochemical[11,12] and fluorescent biosensors.[13] All of the above-mentioned methods are accurate and reliable. However, they are insufficient for screening samples on a large scale. Traditional culture-based methods, as the gold standard methods for *Salmonella* detection and identification, generally need 3–5 days to obtain the results, which is time-consuming.[14] ELISA and PCR can evidently shorten the assay time compared with the culture-based method. However, their inherently time-consuming sample pre-treatments and complicated operations limit their applications in resource-poor districts.[2,15] Electrochemical and fluorescent biosensors are highly selective and sensitive. Due to the sophisticated and costly instruments needed in the assays, these biosensors are still laboratory-based methods. Therefore, there is an urgent demand for highly sensitive, specific, compact, fast, and convenient detection assays for the real-time screening of foodborne pathogens to prevent further spread of foodborne pathogens *via* contaminated food.

These demands subsequently led to a lateral flow immunoassay (LFIA), the most prominent rapid affordable detection assay.[16–18] To date, LFIA has been used to detect a large range

[a]*Hubei Key Laboratory of Environmental and Health Effects of Persistent Toxic Substances, Institute of Environment and Health, Jianghan University, Wuhan, 430056, China. E-mail: hujiao@whu.edu.cn*
[b]*Institute of Medical Engineering, Department of Biophysics, School of Basic Medical Sciences, Xi'an Jiaotong University Health Science Center, Xi'an, 710061, China. E-mail: liucui.tree@163.com*
[c]*Wuhan Academy of Agricultural Sciences, Wuhan, 430072, China*
[d]*Department of Laboratory Medicine, Wuhan Children's Hospital (Wuhan Maternal and Child Healthcare Hospital), Tongji Medical College, Huazhong University of Science & Technology, Wuhan, 430016, China*
[e]*Hubei Provincial Center for Disease Control and Prevention, Wuhan, 430072, China*
†Electronic supplementary information (ESI) available. See DOI: 10.1039/d0an00035c

of biomarkers including proteins, nucleic acids and even whole cells.[19–21] Although it meets many of these criteria, its sensitivity is generally limited by the labels, which act as the signal reporters of LFIA. Currently, colloidal gold is commonly used as a detector reagent in LFIA for the visualization of signals.[22] However, the sensitivity of colloidal gold is insufficient because the emergence of signals relies on the localized surface plasmon resonance of colloidal gold. Besides, colorimetry-based LFIA can only realize qualitative or semi-quantitative detection. With the development of nanotechnology, various nanomaterials have recently emerged as promising signal reporters for LFIA, such as silver nanoparticles,[23] up-conversion phosphors,[24] dyed beads,[25,26] quantum dots (QDs)[27] and magnetic beads.[28,29] QDs as fluorescent nanocrystals have shown unique fluorescence properties, in particular strong and stable fluorescence signals.[30] Notably, the fluorescence intensity is proportional to their concentration, which can realize the quantitative detection of targets.[31,32] Excellent QDs were synthesized using high-temperature growth routes. For biological applications, hydrophobic QDs must be transferred to the aqueous phase; nonetheless, the application of hydrophilic QDs in biology is still limited by colloidal stability after the phase transfer procedure.[33]

In this work, based on quantum dots, we fabricated fluorescent nanobeads (QDNS) by employing polymer nanobeads as carriers to assemble QDs layer by layer. QDNS not only inherited the convenient manipulation ability and colloid stability of polymer nanobeads, but also showed the excellent fluorescence properties of QDs. By employing QDNS as the signal reporter and *Salmonella typhimurium* (*S. typhi*) as a model pathogen, a sensitive, quantitative and robust LFIA was developed for *Salmonella* detection. As schematically illustrated in Fig. 1, generally, if the target pathogen is in a sample, it will be labelled with immuno-QDNS (IQDNS) and then will be captured on the test line to generate a positive result. In this case, the 'T' and 'C' fluorescence lines can be seen simultaneously. If no target bacterium is present, a negative result is obtained, in which only the 'C' line can be seen with an ultraviolet lamp. This is because only IQDNS will be bound to the control line. The results from the reaction membrane are quality interpreted as the presence or absence of a fluorescence signal in the test line, which is read by the naked eye with a portable ultraviolet lamp excitation. Quantitative detection could be realized, which required only a smartphone as the apparatus with simple data processing.

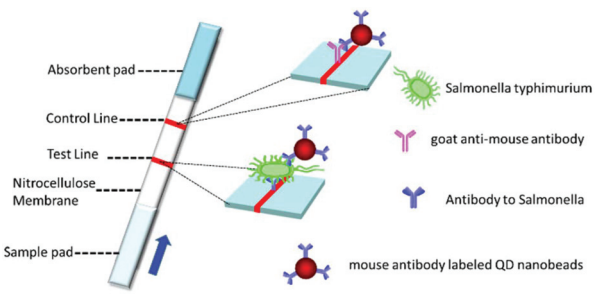

Fig. 1 Schematic diagram of *Salmonella typhimurium* detection by a QDNS-based biosensor.

Experimental section

Materials

ZnCdSe/ZnS Quantum dots (610 nm) were purchased from JiaYuan Quantum Dots Co., Ltd (Wuhan). Mouse antibody to *Salmonella typhimurium* was obtained from Abcam. Goat anti-mouse antibody, FITC-labelled goat anti-mouse IgG, *N*-hydroxysuccinimide (NHS), *N*-(3-(dimethylamino)propyl-*N*′-ethylcarbodiimide hydrochloride (EDC), tetraethyl orthosilicate (TEOS), (3-aminopropyl)triethoxysilane (APTES), and branched poly(ethylene imine) (MW: 25 kDa and 750 kDa) were purchased from Sigma-Aldrich. All other chemical reagents were purchased from Sinopharm Chemical Reagent Co., Ltd (Shanghai). Nitrocellulose membrane, sample pad, absorbent pad, and plastic adhesive card were purchased from JieYi BioTech Co., Ltd (Shanghai). *Salmonella typhimurium*, *Escherichia coli* and *Staphylococcus aureus* were provided by Hubei Provincial Center for Disease Control and Prevention. They were both stored with 50% glycerol at −20 °C and revived on Luria–Bertani (LB) agar plates at 37 °C for 24 h.

Synthesis of quantum dot nanobeads

Carboxylated poly(styrene/acrylamide) copolymer nanospheres (PSt-AAm-COOH) were used as templates to assemble QDs layer-by-layer.[34] First, 20 mg of Pst-AAm-COOH was reacted with branched poly(ethylene imine) (PEI, 0.2 g, MW: 25 kDa) under EDC activated in 2.4 mL phosphate-buffered saline buffer solution (PBS, 0.01 M, pH 7.2) for 4 h at 25 °C with a gentle shaking of 150 rpm. Then, the solution was centrifugated and the precipitate was washed with 1.6 mL NaCl (0.5 M) and ultrapure water in turn to get PEI-modified nanospheres. Second, PEI-modified nanospheres were dehydrated with absolute ethyl alcohol and then reacted with 1 mg hydrophobic QDs in 1.6 mL hexanol for 2 h at 25 °C with a gentle shaking of 150 rpm. Then, the solution was washed to remove excess QDs and reacted with 16 mg branched poly(ethylene imine) (MW: 750 kDa) in 1.6 mL PBS (0.01 M, pH 7.2) for 2 h at 25 °C with a gentle shaking of 150 rpm. After repeating the assembly process of QDs and PEI three times, the nanospheres were treated with tetraethylorthosilicate and (3-aminopropyl) triethoxysilane to get an outer layer of silica shell to increase the stability of the QDs. Through further modification with succinic anhydride, carboxyl-modified QDNS were obtained.

Preparation of antibody-labelled quantum dot nanobeads

Two mg QDNS were washed with 400 μL PBS (0.01 M, pH 6.8) three times and resuspended in 200 μL PBS (0.01 M, pH 6.8). Then, 100 μL EDC (5 mg mL^{-1}) and 100 μL NHS (2.5 mg mL^{-1}) were added into the QDNS solution. After gentle shaking for 20 min, the active QDNS were centrifuged and washed with 400 μL PBS (0.01 M, pH 7.2) three times. The precipitate was

resuspended with 400 μL PBS (0.01 M, pH 7.2) and 20 μg antibodies to *Salmonella* were added. After reacting for 4 h at 25 °C, the resultant antibody-labelled QDNS (immuno-QDNS) were washed and dispersed in 100 μL PBS (0.01 M, pH 7.2) at 4 °C for further use.

Bacteria culture

Salmonella typhimurium (ATCC 14028), *Staphylococcus aureus* (CCTCC AB91093) and *Escherichia coli* (CCTCC AB 2012883) were grown in Luria–Bertani broth at 37 °C for 24 h. To get the exact concentration of bacteria, colonies were picked to prepare bacterial suspensions with 0.9% NaCl. Then, 10 μL of proper dilution was plated onto the culture plate and incubated at 37 °C for 24 h to count the colonies to get the number of colony forming units per millilitre (CFU mL^{-1}). Simultaneously, the same bacterial concentrations of *S. typhi* and other bacteria were diluted in broth or buffer (1× PBS containing 1% BSA and 1% Tween-20) to get a serial dilution of bacterial suspensions.

Preparation of QDNS-based lateral flow immunoassay

The QDNS-based lateral flow test strip consists of the following components: sample pad, conjugate pad, nitrocellulose membrane, absorbent pad and plastic adhesive card. Sample pad, conjugate pad, nitrocellulose membrane and absorbent pad were assembled onto the plastic adhesive card in turn. Each part overlapped 2 mm to ensure that the solution could migrate through the strip during the assay. Antibodies to *S. typhi* and goat anti-mouse IgG solutions were dispensed on the nitrocellulose membrane to form the test and control zones, respectively. After dispensing, the card was dried at 37 °C for 1 h and cut into 3 mm width strips.

Detection of *S. typhi* in buffer and broth

One mL buffer or broth sample containing *S. typhi* was centrifugated at 12 000 rpm for 2 min and resuspended with 50 μL of 1% BSA-Tween 20 in 1× PBS. Then, 3 μL antibody-labelled QDNS were added into the solution. After mixing with a vortex for about 10 s, the solution containing QDNS-labelled *S. typhi* and free QDNS was added onto the sample pad. The fluorescence line could be observed with a portable ultraviolet lamp as soon as the liquid flowed through the test line and control line. After waiting for 10 min, the fluorescence intensity of the test line was collected and analysed with a smartphone as the apparatus with simple data processing. Briefly, for quantitative detection, the obtained image was easily transferred to RGB intensity and the red-channel intensity was extracted with the photoshop software to quantify the fluorescence intensity.

Results and discussion

Characterizations of QDNS and IQDNS

In our previous work, QDNS were fabricated by an embedding method, and they exhibited high intensity.[35] Limited to the inner space of the polymer nanosphere, only about 340 quantum dots were embedded into one polymer nanosphere. Herein, taking advantage of the red quantum dots shown in Fig. 2A, QDNS were fabricated by the layer-by-layer assembly method and embedding method. As shown in Fig. 2B, QDNS fabricated with the layer-by-layer assembly method are monodispersed with a rough surface. The inset image in Fig. 2B shows the TEM image of QDNS without silylanization treatment. A comparison of the two images indicates that the silica shell has been fabricated successfully. Moreover, QDNS exhibited excellent fluorescence properties of QDs (Fig. 2C) and showed superiority in fluorescence intensity over QDs (Fig. S1A†). Additionally, the fluorescence intensities of the three batches of QDNS were nearly the same (Fig. S1B†). The results suggested that the reproducibility of the layer-by-layer method was very high.

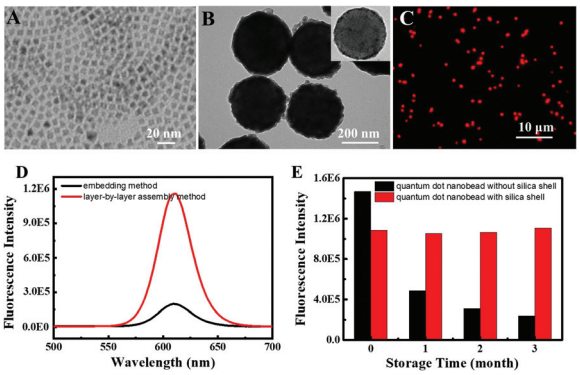

Fig. 2 (A) TEM image of red quantum dots. (B) TEM image of carboxyl-modified QDNS. Inset: TEM image of QDNS without silica shell. (C) Fluorescence microscopic image of QDNS. (D) Fluorescence intensity of QDNS (black line, fabricated by the embedding method) and QDNS (red line, fabricated by the layer-by-layer assembly method) at the same particle concentrations. (E) Fluorescence intensity of QDNS with/without silica shell during three month storage.

Compared with our previous work,[35] the fluorescence of QDNS fabricated by the layer-by-layer assembly method was much higher than that of QDNS fabricated using the embedding method (Fig. 2D). This was because much more QDs were coated on one polymer nanosphere. From Fig. 2E, we can find 90% decrease in the fluorescence intensity of QDNS without silica shells after storage for three months (black column). In contrast, the fluorescence intensity of QDNS decreased slightly during the silylanization treatment (red column). This suggested that the silica shell indeed increased the stability of QDs.

Then, QDNS were modified with mouse antibodies to *S. typhi*. FITC-labelled goat anti-mouse IgG was used to verify antibody conjugation. After being modified with mouse antibodies, QDNS exhibited green fluorescence of FITC and red fluorescence of QDs simultaneously. As shown in Fig. S2,† the microscopy images demonstrate the successful fabrication of QDNS-antibody conjugates (IQDNS).

Proof-of-concept assay for the detection of *S. typhi*

To demonstrate the feasibility of the QDNS-based LFIA for *S. typhi* detection, the biosensor was used to detect *S. typhi* in

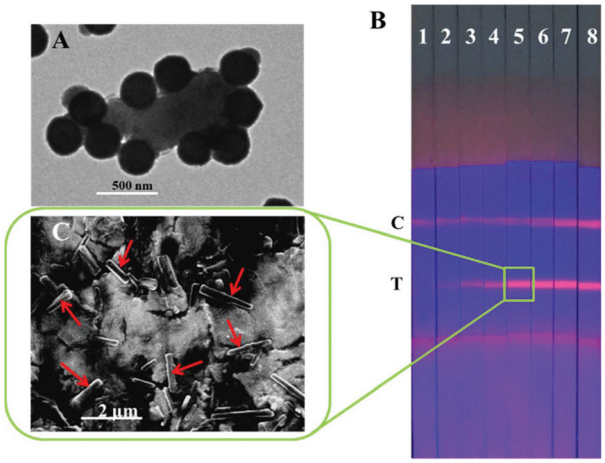

Fig. 3 (A) Typical TEM image of the *S. typhi* labelled by QDNS. (B) Typical fluorescence pictures of the test strips for 0, 5×10^3, 1×10^4, 5×10^4, 1×10^5, 5×10^5, 1×10^6 and 5×10^6 CFU mL^{-1} *S. typhi* in buffer. (C is the control line; T is the test line; 1 to 8 indicate the concentrations of *S. typhi* from 0 to 5×10^6 CFU mL^{-1}). (C) Typical SEM image of the QDNS-based biosensor in the presence of *S. typhi* (10^5 CFU mL^{-1}).

buffer under optimized detection conditions (Fig. S3†). The TEM image (Fig. 3A) shows that many IQDNS are bound to *S. typhi* after simple mixing. This indicated that the bonding capability between IQDNS and *S. typhi* was strong. A series of *S. typhi* suspensions with different concentrations were tested with this method. As expected from the original design, no red fluorescence was observed on the test line in the absence of *S. typhi* (Fig. 3B, '1') because no *S. typhi*/QDNS complex occurred on the test line. When *S. typhi* was present in a sample, two red fluorescence lines were observed on the test line and control line simultaneously (Fig. 3B, '2–8'). It could be observed that the test line started to appear at 5×10^3 CFU mL^{-1} (Fig. 3B, '2'). The fluorescence intensity on the test line increased on increasing the *S. typhi* concentration. This observation is attributed to the emergence of QDNS captured on the test line and control line. In this case, *S. typhi* can be clearly identified on the test line with SEM (Fig. 3C). These results demonstrated that *S. typhi* can be detected by QDNS-based LFIA visually.

Analytical performance of QDNS-based LFIA for *S. typhi* detection

Due to the low infectious dose of *Salmonella* (10 cells), incubation of samples to improve the number of pathogens in the broth is very important and necessary. Herein, we spiked *S. typhi* in the Luria–Bertani broth to mimic the practice samples after incubation. Hence, a series of experiments were conducted using various concentrations of *S. typhi* in broth ranging from 0 to 10^7 CFU mL^{-1}. As shown in Fig. 4A, the results are comparable to those of the buffer samples. For the blank broth sample, only free QDNS were captured on the control line. For all strips of positive samples, two lines appeared except for 10^4 CFU mL^{-1} and the test line started to

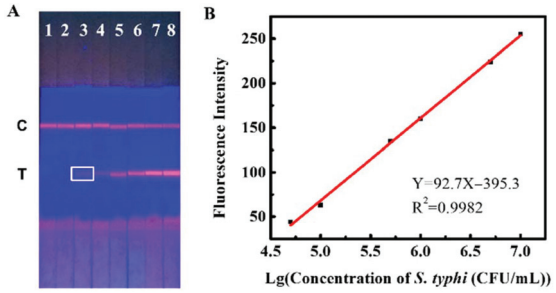

Fig. 4 (A) Typical fluorescence pictures of the test strips for 0, 10^4, 5×10^4, 10^5, 5×10^5, 10^6, 5×10^6 and 10^7 CFU mL^{-1} *S. typhi* in broth. (C is the control line; T is the test line; white box shows the detection limit; 1 to 8 indicate the concentrations from 0 to 10^7 CFU mL^{-1}). (B) QDNS-based biosensor linear response for detection of *Salmonella* in the concentration range of 5×10^4–10^7 CFU mL^{-1} in broth.

appear at 5×10^4 CFU (indicated by the white box). The quantification of signal intensities (Fig. 4B) showed that the fluorescence intensity was proportional to the concentration of the bacteria and that the limit of detection was calculated to be 4.2×10^4 CFU mL^{-1}.

Although the sensitivity was not too high compared with that of some other reported methods (Table 1), the assay presented herein exhibited balanced sensitivity, speed and quantitative ability. Additionally, compared with some other label-based LFIA for bacteria detection, QDNS-based LFIA showed superiority in sensitivity. These results demonstrate that QDNS are excellent labels and they hold great potential for the sensitive detection of other foodborne pathogens.

Evaluating the reliability and specificity of the assay

To evaluate the analytical specificity and selectivity of the assay, mixed broth samples containing 5×10^5 CFU mL^{-1} *S. typhi* and 1.5×10^7 CFU mL^{-1} *Escherichia coli* (*E. coli*) or *Staphylococcus aureus* (*S. aureus*) were tested using this method. As shown in Fig. 5, only the samples containing *S. typhi* exhibit two bright fluorescence lines, and other samples only show control lines, indicating the excellent specificity and selectivity of the assay.

To further validate the accuracy, reliability and possibility of the QDNS-based LFIA for practical sample detection, a single-blind trial of 50 broth samples of *S. typhi* was performed. Here, 50 broth samples (10 negative samples and 40 positive samples with different concentrations of *S. typhi*) were randomly assigned and detected by 10 testers with our method within 15 min. The results indicated 40 samples as positive and 10 samples as negative (Table 2). This result had a high coincidence of 100% with the expected results, indicating the high accuracy of the assay. The short assay time suggests that the assay is a favourable method for the rapid screening of a large number of samples.

Table 1 Summary of the analytical performances of the detection of *Salmonella* with different methods

Method	Target	Label	Detection limit (CFU mL^{-1})	Assay time	Linearity range	Ref.
SPR[a]	*Salmonella* sp.	Gold nanoparticles	7400	80 min	10^3–10^6	36
PADs[b]	*Salmonella typhimurium*	β-Galactosidase	10^2	75 min	Qualitative	5
Thermal sensor	*Salmonella typhimurium*	Magnetic nanomaterials	300	1.5 h	300–10^3	37
Optical biosensor	*Salmonella typhimurium*	Fluorescent nanospheres	10	>1 h	10^5–10^7	32
LFIA[c]	*Salmonella enteritidis*	Gold nanoparticles	10^7		Qualitative	38
LFIA	*Salmonella enteritidis*	Magnetic nanospheres	1.95×10^6	30 min	Qualitative	39
LFIA	*Salmonella enteritidis*	Gold magnetic bifunctional nanobeads	5×10^5		Qualitative	40
Two-step LFIA[d]	*Salmonella choleraesuis*	Fluorescent microspheres	1.5×10^5	>70 min	7.6×10^4–7.6×10^6	41
LFIA	*S. typhi.*	Colorimetric-fluorescent-magnetic nanosphere	3.5×10^3	35 min	1.88×10^4–1.88×10^7	29
LFIA	*S. typhi.*	Up-coversion phosphor	10^4	20 min	10^4–10^7	42
LFIA	*S. typhi*	Quantum dot nanobeads	5×10^3	12 min	5×10^4–10^7	This work

[a] SRP: surface Raman scattering. [b] PADs: paper-based analytical devices. [c] LFIA: lateral flow immunoassay. [d] Two-step LFIA: consists of magnetic separation and chromatography.

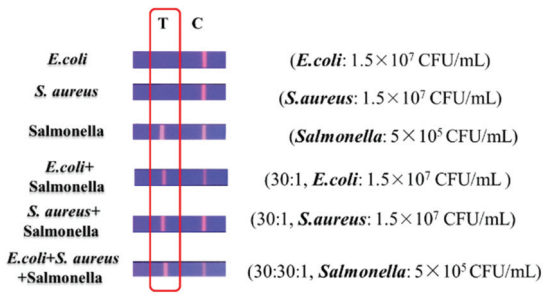

Fig. 5 Specificity and selectivity of the QDNS-based LFIA in mixed broth samples containing 5×10^5 CFU mL^{-1} *S. typhi* and 1.5×10^7 CFU mL^{-1} non-*Salmonella*

Table 2 Determination results of *S. typhi* in spiked broth samples. 'Yes' indicates that the tester was able to observe 'T' and 'C' simultaneously and 'No' indicates that only 'C' line was observed

	Concentration (CFU mL^{-1})					
Tester no.	0	5×10^4	10^5	10^6	10^7	Accuracy (100%)
1	No	Yes	Yes	Yes	Yes	100%
2	No	Yes	Yes	Yes	Yes	100%
3	No	Yes	Yes	Yes	Yes	100%
4	No	Yes	Yes	Yes	Yes	100%
5	No	Yes	Yes	Yes	Yes	100%
6	No	Yes	Yes	Yes	Yes	100%
7	No	Yes	Yes	Yes	Yes	100%
8	No	Yes	Yes	Yes	Yes	100%
9	No	Yes	Yes	Yes	Yes	100%
10	No	Yes	Yes	Yes	Yes	100%

Conclusions

In summary, a sensitive, specific and accurate lateral flow immunoassay has been successfully designed for *S. typhi* detection by employing quantum dot nanospheres (QDNS) as signal reporters. The QDNS inherited the excellent fluorescence properties of QDs and surpassed QDs in colloid stability and manipulation ability. Due to the protection of the silica shell, the fluorescence intensity of QDNS was stable, and this enabled the reproducibility of the assay. Due to the very strong fluorescence of the signal reporter, the detection limit was 5×10^3 CFU mL^{-1} in buffer and 5×10^4 CFU mL^{-1} in broth, and it was 4–40 fold sensitive than commercial LFIA for *Salmonella* detection. It also showed superiority in sensitivity than colloidal gold, gold magnetic nanobeads, and magnetic nanospheres as signal reporters. In addition, the assay exhibited excellent specificity and selectivity. The fluorescence intensity was obvious in the presence of *S. typhi* in the samples even when the concentration of nontarget bacteria was 30-fold that of *S. typhi*. Furthermore, the assay balanced the performance of simplicity, speed, sensitivity and accuracy. The results of 50 single blind tests by 10 testers demonstrated high accuracy of the assay. Given the high sensitivity and accuracy of the assay, our approach provides new opportunities for the detection of *Salmonella* typhimurium in both clinical laboratory and food industry, particularly in combination with POC platforms.

Conflicts of interest

There are no conflicts to declare.

Acknowledgements

This work was supported by the National Natural Science Foundation of China (21804103 and 21805021), China Postdoctoral Science Foundation Funded Project (2018M631057) and the Open Funding Project of Key Laboratory of Analytical Chemistry for

Biology and Medicine (Ministry of Education) (ACBM2019009), the General Program of Health and Family Planning Commission of Hubei Province of China (WJ2017M194), the General Program of Natural Science Foundation of Hubei Province of China (2017CFB709), the Frontier Project of Application Foundation of Wuhan Science and Technology Bureau of China (2018060401011314).

Notes and references

1 G. Taubes, The Bacteria Fight Back, *Science*, 2008, **321**, 356–361.
2 J. R. Andrews and E. T. Ryan, Diagnostics for Invasive Salmonella Infections: Current Challenges and Future Directions, *Vaccine*, 2015, **33**, C8–C15.
3 N. Cheng, Y. Song, M. M. A. Zeinhom, Y. C. Chang, L. Sheng, H. Li, D. Du, L. Li, M. J. Zhu, Y. Luo, W. Xu and Y. Lin, Nanozyme-Mediated Dual Immunoassay Integrated with Smartphone for Use in Simultaneous Detection of Pathogens, *ACS Appl. Mater. Interfaces*, 2017, **9**, 40671–40680.
4 S. M. Crim, M. Iwamoto, J. Y. Huang, P. M. Griffin, D. Gilliss, A. B. Cronquist, M. Cartter, M. Tobin-D'Angelo, D. Blythe, K. Smith, *et al.*, Incidence and Trends of Infection with Pathogens Transmitted Commonly Through Food - Foodborne Diseases Active Surveillance Network, 10 US Sites, 2006-2013, *MMWR Morb. Mortal. Wkly. Rep.*, 2014, **63**, 328–332.
5 M. Srisa-Art, K. E. Boehle, B. J. Geiss and C. S. Henry, Highly Sensitive Detection of Salmonella typhimurium Using a Colorimetric Paper-Based Analytical Device Coupled with Immunomagnetic Separation, *Anal. Chem.*, 2018, **90**, 1035–1043.
6 N. Kumar, Y. Hu, S. Singh and B. Mizaikoff, Emerging biosensor platforms for the assessment of water-borne pathogens, *Analyst*, 2018, **143**, 359–373.
7 F. Tang, D. W. Pang, Z. Chen, J. B. Shao, L. H. Xiong, Y. P. Xiang, Y. Xiong, K. Wu, H. W. Ai, H. Zhang, X. L. Zheng, J. R. Lv, W. Y. Liu, H. B. Hu, H. Mei, Z. Zhang, H. Sun, Y. Xiang and Z. Y. Sun, Visual and efficient immunosensor technique for advancing biomedical applications of quantum dots on Salmonella detection and isolation, *Nanoscale*, 2016, **8**, 4688–4698.
8 X. Zhao, C. W. Lin, J. Wang and D. H. Oh, Advances in Rapid Detection Methods for Foodborne Pathogens, *J. Microbiol. Biotechnol.*, 2014, **24**, 297–312.
9 T. Wei, D. Du, M.-J. Zhu, Y. Lin and Z. Dai, An Improved Ultrasensitive Enzyme-Linked Immunosorbent Assay Using Hydrangea-Like Antibody–Enzyme–Inorganic Three-in-One Nanocomposites, *ACS Appl. Mater. Interfaces*, 2016, **8**, 6329–6335.
10 N. Khemthongcharoen, W. Wonglumsom, A. Suppat, K. Jaruwongrungsee, A. Tuantranont and C. Promptmas, Piezoresistive Microcantilever-Based DNA Sensor for Sensitive Detection of Pathogenic Vibrio Cholerae O1 in Food Sample, *Biosens. Bioelectron.*, 2015, **63**, 347–353.
11 Z. Yang, Y. Wang and D. Zhang, A novel multifunctional electrochemical platform for simultaneous detection, elimination, and inactivation of pathogenic bacteria based on the Vancomycin-functionalised AgNPs/3D-ZnO nanorod arrays, *Biosens. Bioelectron.*, 2017, **98**, 248–253.
12 M. Xu, R. Wang and Y. Li, An electrochemical biosensor for rapid detection of E. coli O157:H7 with highly efficient bifunctional glucose oxidase-polydopamine nanocomposites and Prussian blue modified screen-printed interdigitated electrodes, *Analyst*, 2016, **141**, 5441–5449.
13 L. Chen, X. Li, T. Zou, T. Wang, X. Cui, Y. Chen, C. Zhang and S. Zhao, Ultrasensitive detection of H. pylori in human feces based on immunomagnetic bead capture and fluorescent quantum dots, *Analyst*, 2019, **144**, 4086–4092.
14 Q. Gan, X. Wang, Y. Wang, Z. Xie, Y. Tian and Y. Lu, Culture-Free Detection of Crop Pathogens at the Single-Cell Level by Micro-Raman Spectroscopy, *Adv. Sci.*, 2017, **4**, 1700127.
15 H. Sharma and R. Mutharasan, Review of Biosensors for Foodborne Pathogens and Toxins, *Sens. Actuators, B*, 2013, **183**, 535–549.
16 E. B. Bahadır and M. K. Sezgintürk, Lateral Flow Assays: Principles, Designs and Labels, *TrAC, Trends Anal. Chem.*, 2016, **82**, 286–306.
17 M. J. Raeisossadati, N. M. Danesh, F. Borna, M. Gholamzad, M. Ramezani, K. Abnous and S. M. Taghdisi, Lateral Flow Based Immunobiosensors for Detection of Food Contaminants, *Biosens. Bioelectron.*, 2016, **86**, 235–246.
18 Q. Ju, M. O. Noor and U. J. Krull, Paper-Based Biodetection Using Luminescent Nanoparticles, *Analyst*, 2016, **141**, 2838–2860.
19 H. Shen, F. Xu, M. Xiao, Q. Fu, Z. Cheng, S. Zhang, C. Huang and Y. Tang, A new lateral-flow immunochromatographic strip combined with quantum dot nanobeads and gold nanoflowers for rapid detection of tetrodotoxin, *Analyst*, 2017, **142**, 4393–4398.
20 X. Ge, A. M. Asiri, D. Du, W. Wen, S. Wang and Y. Lin, Nanomaterial-enhanced paper-based biosensors, *TrAC, Trends Anal. Chem.*, 2014, **58**, 31–39.
21 M. Chen, Z. Yu, D. Liu, T. Peng, K. Liu, S. Wang, Y. Xiong, H. Wei, H. Xu and W. Lai, Dual Gold Nanoparticle Lateflow Immunoassay for Sensitive Detection of Escherichia coli O157:H7, *Anal. Chim. Acta*, 2015, **876**, 71–76.
22 D. Quesada-González and A. Merkoçi, Nanoparticle-Based Lateral Flow Biosensors, *Biosens. Bioelectron.*, 2015, **73**, 47–63.
23 C. W. Yen, H. de Puig, J. O. Tam, J. Gomez-Marquez, I. Bosch, K. Hamad-Schifferli and L. Gehrke, Multicolored silver nanoparticles for multiplexed disease diagnostics: distinguishing dengue, yellow fever, and Ebola viruses, *Lab Chip*, 2015, **15**, 1638–1641.
24 M. You, M. Lin, Y. Gong, S. Wang, A. Li, L. Ji, H. Zhao, K. Ling, T. Wen, Y. Huang, D. Gao, Q. Ma, T. Wang, A. Ma,

X. Li and F. Xu, Household Fluorescent Lateral Flow Strip Platform for Sensitive and Quantitative Prognosis of Heart Failure Using Dual-Color Upconversion Nanoparticles, *ACS Nano*, 2017, **11**, 6261–6270.

25 X. L. Huang, Z. P. Aguilar, H. M. Li, W. H. Lai, H. Wei, H. Y. Xu and Y. H. Xiong, Fluorescent Ru(phen)(3)(2+)-Doped Silica Nanoparticles-Based ICTS Sensor for Quantitative Detection of Enrofloxacin Residues in Chicken Meat, *Anal. Chem.*, 2013, **85**, 5120–5128.

26 W. Sheng, S. Li, Y. Liu, J. Wang, Y. Zhang and S. Wang, Visual and rapid lateral flow immunochromatographic assay for enrofloxacin using dyed polymer microspheres and quantum dots, *Microchim. Acta*, 2017, **184**, 4313–4321.

27 Z. H. Li, Y. Wang, J. Wang, Z. W. Tang, J. G. Pounds and Y. H. Lin, Rapid and Sensitive Detection of Protein Biomarker Using a Portable Fluorescence Biosensor Based on Quantum Dots and a Lateral Flow Test Strip, *Anal. Chem.*, 2010, **82**, 7008–7014.

28 D.-B. Wang, B. Tian, Z.-P. Zhang, X.-Y. Wang, J. Fleming, L.-J. Bi, R.-F. Yang and X.-E. Zhang, Detection of Bacillus Anthracis Spores by Super-Paramagnetic Lateral-Flow Immunoassays Based on "Road Closure", *Biosens. Bioelectron.*, 2015, **67**, 608–614.

29 J. Hu, Y. Z. Jiang, M. Tang, L. L. Wu, H. Y. Xie, Z. L. Zhang and D. W. Pang, Colorimetric-Fluorescent-Magnetic Nanosphere-Based Multimodal Assay Platform for Salmonella Detection, *Anal. Chem.*, 2019, **91**, 1178–1184.

30 Ü. Dogan, E. Kasap, D. Cetin, Z. Suludere, I. H. Boyaci, C. Türkyılmaz, N. Ertas and U. Tamer, Rapid Detection of Bacteria Based on Homogenous Immunoassay Using Chitosan Modified Quantum Dots, *Sens. Actuators, B*, 2016, **233**, 369–378.

31 J. Hu, C. Y. Wen, Z. L. Zhang, M. Xie, M. Wu and D. W. Pang, Optically Encoded Multifunctional Nanospheres for One-Pot Separation and Detection of Multiplex DNA Sequences, *Anal. Chem.*, 2013, **85**, 11929–11935.

32 C. Y. Wen, J. Hu, Z. L. Zhang, Z. Q. Tian, G. P. Ou, Y. L. Liao, Y. Li, M. Xie, Z. Y. Sun and D. W. Pang, One-step sensitive detection of Salmonella typhimurium by coupling magnetic capture and fluorescence identification with functional nanospheres, *Anal. Chem.*, 2013, **85**, 1223–1230.

33 C. N. Zhu, P. Jiang, Z. L. Zhang, D. L. Zhu, Z. Q. Tian and D. W. Pang, Ag(2)Se quantum dots with tunable emission in the second near-infrared window, *ACS Appl. Mater. Interfaces*, 2013, **5**, 1186–1189.

34 M. Xie, J. Hu, C. Y. Wen, Z. L. Zhang, H. Y. Xie and D. W. Pang, Fluorescent-Magnetic Dual-Encoded Nanospheres: a Promising Tool for Fast-Simultaneous-Addressable High-Throughput Analysis, *Nanotechnology*, 2012, **23**, 035602.

35 J. Hu, Z. L. Zhang, C. Y. Wen, M. Tang, L. L. Wu, C. Liu, L. Zhu and D. W. Pang, Sensitive and Quantitative Detection of C-Reaction Protein Based on Immunofluorescent Nanospheres Coupled with Lateral Flow Test Strip, *Anal. Chem.*, 2016, **88**, 6577–6584.

36 H. Vaisocherova-Lisalova, I. Visova, M. L. Ermini, T. Springer, X. C. Song, J. Mrazek, J. Lamacova, N. S. Lynn, P. Sedivak and J. Homola, Low-fouling surface plasmon resonance biosensor for multi-step detection of foodborne bacterial pathogens in complex food samples, *Biosens. Bioelectron.*, 2016, **80**, 84–90.

37 Z. Zhang, Q. Wang, L. Han, S. Du, H. Yu and H. Zhang, Rapid and sensitive detection of Salmonella typhimurium based on the photothermal effect of magnetic nano-materials, *Sens. Actuators, B*, 2018, **268**, 188–194.

38 R. K. Gast, P. S. Holt, M. S. Nasir, M. E. Jolley and H. D. Stone, Detection of Salmonella enteritidis in incubated pools of egg contents by fluorescence polarization and lateral flow immunodiffusion, *Poult. Sci.*, 2003, **82**, 687–690.

39 M.-L. Duan, Y.-M. Huang, S.-S. Wu, G.-Q. Li, S.-Y. Wang, M.-H. Chen, C. Wang, D.-F. Liu, C.-W. Liu and W.-H. Lai, Rapid and sensitive detection of Salmonella enteritidis by a pre-concentrated immunochromatographic assay in a large-volume sample system, *RSC Adv.*, 2017, **7**, 55141–55147.

40 S. Q. Xia, Z. B. Yu, D. F. Liu, C. L. Xu and W. H. Lai, Developing a Novel Immunochromatographic Test Strip with Gold Magnetic Bifunctional Nanobeads (GMBN) for Efficient Detection of Salmonella Choleraesuis in Milk, *Food Control*, 2016, **59**, 507–512.

41 Z. Huang, S. Q. Xia, D. F. Liu, C. W. Liu and W. H. Lai, Fluorescent Microspheres Lateral Flow Assay Based on Immunomagnetic Separation for Detection of S. choleraesuis, *Chin. J. Anal. Chem.*, 2017, **45**, 217–223.

42 Y. Zhao, H. Wang, P. Zhang, C. Sun, X. Wang, X. Wang, R. Yang, C. Wang and L. Zhou, Rapid Multiplex Detection of 10 Foodborne Pathogens with an Up-Converting Phosphor Technology-Based 10-Channel Lateral Flow Assay, *Sci. Rep.*, 2016, **6**, 21342.